J Clust Sci
DOI 10.1007/s10876-014-0815-0

ORIGINAL PAPER

Adsorption of Formic Acid and Formate Anion on ZnO Nanocage: A DFT Study

Hamid Salimi · Ali Ahmadi Peyghan · Maziar Noei

Received: 2 December 2013

Abstract By using density functional calculations, we studied the adsorption of formic acid and formate anion on a $Zn_{12}O_{12}$ nanocage in terms of energetic, electronic and geometric properties. The adsorption of *cis*- and *trans*-formic acids on the cluster is accompanied by release of energies in the range of 7.37–36.11 kcal/mol. The adsorption of *trans*-formic acid was found to be much more favorable than the *cis*-acid. It was also shown that the *trans*-formic acid can be dissociated to H^+ cation and formate anion on the cluster surface, releasing energy of 28.08 kcal/mol. Adsorption of formate anion was found to be much more favorable than formic acids. In contrast to formic acid, the formate anion significantly influences the electronic properties of the cluster by decreasing HOMO–LUMO gap and work function. The decrement in the work function indicates that the field electron emission from the cluster surface is facilitated upon the formate adsorption.

Keywords ZnO nanocluster · DFT · Adsorption · Computational study

Introduction

Zinc oxide (ZnO) can be in bulk or nanostructure morphologies such as nanotubes, nanowires and clusters [1–3]. Bulk wurtzite structure ZnO is a wide bandgap

H. Salimi
Department of Polymer and Petrochemicals, Standard Research Institute, Karaj, Iran

A. Ahmadi Peyghan (✉)
Young Researchers and Elite Club, Central Tehran Branch, Islamic Azad University, Tehran, Iran
e-mail: ahmadi.iau@gmail.com

M. Noei
Department of Chemistry, College of Chemical Engineering, Mahshahr Branch, Islamic Azad University, Mahshahr, Iran

Published online: 16 November 2014

semiconductor with a large exciton binding energy of 60 meV at room temperature. It has many applications due to its hardness, chemical stability, and excellent optical and electric properties [4]. It can be used in ultraviolet lasers, solar cells, photocatalysts, field emitters, gas sensors and diluted magnetic semiconductors for spintronics [5, 6]. ZnO nanotubes, nanowires and cluster have also been widely investigated experimentally and theoretically [7, 8]. Recently, research efforts have been devoted to $(XY)_n$, X = Al, B, Mg,…, and Y = N, P, O,…, nanostructures such as nanoclusters, nanohorns, nanotubes, and nanowires [9–12]. The fullerene-like cages $(XY)_{12}$ have been theoretically predicted to be the most stable clusters among different types of $(XY)_n$ structures [13], indicating that fullerene-like cage can be a magic cluster and has inherent special stability when n equals to 12. ZnO nanocluster structures have been widely studied both theoretically and experimentally [14, 15].

The chemistry of semiconducting metal oxide surfaces is industrially important, with many applications, for example, in heterogeneous catalysis, and nanostructured electrochemical devices [16]. The complexity of these surfaces has, however, largely prevented a detailed understanding of these important systems at the molecular level. It is, therefore, an important field of current research. Formic acid was dissociated on metal and metal oxide surfaces at room temperature to give formate anion and surface hydroxyl species [17]. Formic acid adsorbed on the metal and metal oxide surfaces decomposes to produce $H_2O + CO$ or $H_2 + CO_2$ [18]. The adsorption of formic acid, HCO_2H, on ZnO surfaces is of particular importance, both because metal oxides such as ZnO are known to catalyze the decomposition of formic acid and because ZnO-based dye-sensitized electrochemical devices, such as solar cells, are being developed in which carboxylic acid groups are responsible for the dye-surface contact [19].

The adsorption of formic acid on the TiO_2 (110) and (011) surfaces have recently been studied theoretically [20]. Noto et al. studied the dissociative adsorption and decomposition of formic acid on a ZnO surface using infrared spectroscopy, and the structure of the formate ion adsorbed on a ZnO surface was considered to be either bridging or bidentate [21]. Au et al. reported that formic acid is adsorbed on a ZnO (1010) surface and gives formate anion and hydroxyls [22]. Petrie and Vohs studied the reaction of formic acid with the (0001)-Zn surface of ZnO. They reported that molecularly adsorbed formic acid is the major species at 160 K, and it dissociates into the formate anion by heating [23]. In this work, we report a density functional theory (DFT) study of the adsorption of formic acid (FA) and formate anion (FO) on $Zn_{12}O_{12}$ nanocage. The main questions which have been tried to be explored in the present study include: (1) where is the molecule placed upon the interaction? (2) How are the geometric and electronic properties modified by molecule adsorption? and (3) what is the effect of FA and FO adsorption on the electronic properties of $Zn_{12}O_{12}$?

Computational Details

Spin-unrestricted B3LYP hybrid density functional theory (DFT) method within 6-311 ++ G** basis set was used for the optimization, density of states (DOS),

molecular electrostatic potential (MEP) frontier molecular orbitals (FMO) analyses, and energy calculations. It is clear that the second star and plus in 6-311 ++ G** is due to existence of hydrogen atoms in the studied systems. The B3LYP is a commonly used functional for computational study of nanostructure materials [24–29]. With the optimized structures, the adsorption energy (E_{ad}) of the species on the pure cluster is obtained using the following equation:

$$E_{ad} = E(X - Zn_{12}O_{12}) - E(X) - E(Zn_{12}O_{12}) + E(BSSE) \quad (1)$$

where, E (X- $Zn_{12}O_{12}$) is the total energy of radical- $Zn_{12}O_{12}$ complexes, and E ($Zn_{12}O_{12}$) or E (X) refers to the energy of an isolated $Zn_{12}O_{12}$ or FA (FO). The negative value of E_{bin} indicates the exothermic nature of the adsorption. Basis set superposition error (BSSE) was corrected for weak interactions. All calculations were carried out using the GAMESS electronic structure program [30]. The canonical assumption for Fermi level (E_F) is that in a molecule (at T = 0 K) it lies approximately in the middle of the highest occupied molecular orbital (HOMO) and the lowest unoccupied molecular orbital (LUMO) energy gap (E_g). It is noteworthy to mention that, in fact, what lies in the middle of the E_g is the chemical potential, and since the chemical potential of a free gas of electrons is equal to its Fermi level as traditionally defined, the Fermi level of the considered systems is at the center of the E_g.

Results and Discussion

It is well known that the FA in the gas phase is a mixture of *cis* and *trans* forms. Therefore, we should consider that both *trans* and *cis* forms approach the cluster surface. The adsorption of *cis*- and *trans*- FA is described in "Adsorption of Molecular FA on Zn12O12" section. The structure of the adsorbed FO, which has been observed experimentally, is described in "Adsorption of FO Anion on Zn12O12" section. The transformation to the adsorbed FO from molecularly adsorbed *cis*- and *trans*- FA is described in "Dissociation of FA to FO on Zn12O12" section.

Adsorption of Molecular FA on $Zn_{12}O_{12}$

The optimized $Zn_{12}O_{12}$ cluster includes eight six-membered (6MR) and six four-membered rings (4MR) with T_h symmetry. The angles in tetragons and hexagons vary from 88.9° to 90.7° and from 116.1° to 123.5° (Fig. 1), respectively. Two topologically nonequivalent Zn–O bonds are present in $Zn_{12}O_{12}$ cluster; one is shared by two 6-MRs (B_{66}) and the other is shared between a 4- and a 6-MR (B_{64}) with bond lengths of 1.91 and 1.98 Å, respectively.

To determine the minimum energy adsorption structure of FA on the exterior surface of the $Zn_{12}O_{12}$, a number of distinct starting structures were used for optimization. We assume there are three typical structures for molecularly adsorbed *cis*-molecule: bridging, bidentate and unidentate which are shown in Fig. 2 (for FO, which is similar to FA). We tried to find stable structures that could be assigned to these three structures. The plane of FA is kept perpendicular to the ZnO surface to

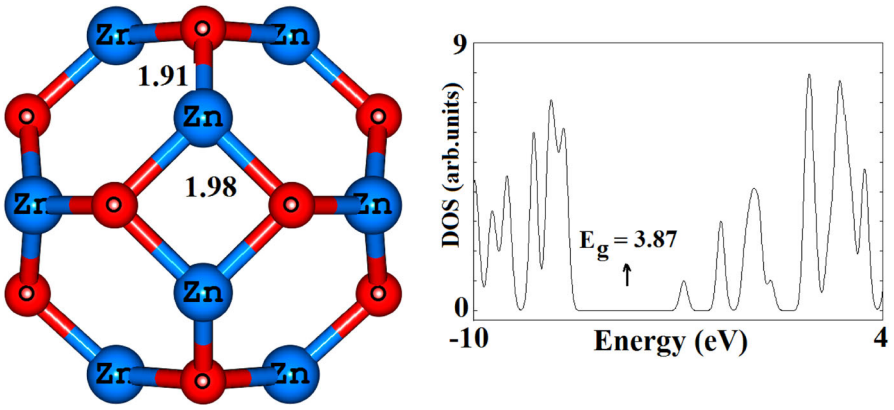

Fig. 1 The optimized structure of $Zn_{12}O_{12}$ and its DOS plot. Bond lengths in Å and angles in degree

optimize the structure. Two optimized geometries of the adsorbed species are shown in Fig. 3. As shown in Fig. 3, configuration P shows the interaction between both of the oxygen atoms of FA molecule and the Zn atoms of a 4-MR of the cluster, namely bridging type interaction. In this configuration, a net charge of about 0.147 electrons is transferred from molecule to the cluster and calculated E_{ad} value is about −7.37 kcal/mol (Table 1) and the smallest distance of molecule to the cluster is about 2.26 Å.

The above results indicate that this interaction is weak and belongs to physisorption category. The other *cis*-FA adsorption yields the configuration Q, in which carboxylate oxygen atom of FA is close to a Zn atom (as unidentate type interaction) by a distance of 2.13 Å. This configuration has an E_{ad} of −11.77 kcal/mol and a charge transfer of 0.311 *e* from the molecule to the cluster. As shown in configurations P and Q, *cis*-FA can be physisorbed on $Zn_{12}O_{12}$, so only its oxygen atoms interact with Zn atom(s) of the cluster. This phenomenon is discussed by MEP and FMO analyses. Based on Mulliken population analysis, the point charge of zinc and oxygen in $Zn_{12}O_{12}$ cluster is +0.424 and −0.424 *e*, respectively, which is in agreement with our calculated MEP. As shown by the mapped-MEP of $Zn_{12}O_{12}$ in Fig. 4a, the Zn atoms are positively charged (blue colors), while the O atoms are negatively charged (red colors) in Zn–O bonding, so it seems that these atoms are suitable sites for nucleophilic attack of FA molecule. As shown in Fig. 4b, calculated lowest unoccupied molecular orbital (LUMO) for $Zn_{12}O_{12}$ cluster reveals that it is more localized on the zinc atoms in the energy level of −3.17 eV. Also, as can be seen in Fig. 4c, the highest occupied molecular orbital (HOMO) of FA molecule is located on the O atoms, thus it prefers to sit on the Zn atom of the cluster from O head.

Other case of FA interaction with $Zn_{12}O_{12}$ is chemisorption, in which *trans*-FA is located perpendicularly on the top of the cluster. The E_{ad} for *trans*-FA addition on the B_{64} bond (−36.11 kcal/mol, configuration S) is more negative than that on the B_{66} bond (−35.81 kcal/mol, configuration R) with rather a significant Mulliken charge transfer from the cluster to the molecule for both of them (Fig. 5). It is may be due to the above mentioned fact that the B_{64} bond is shared between 4- and 6-MRs, but the

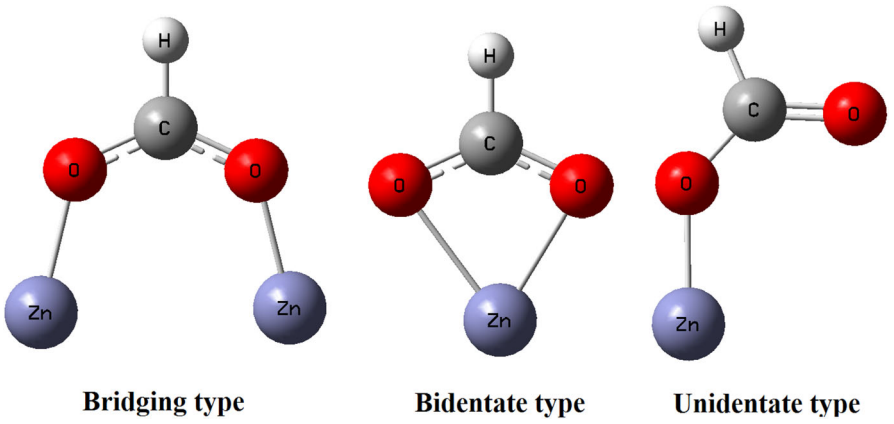

Fig. 2 Three possible geometries for the FO anion on the surface

B_{66} bond is shared between two 6-MRs; therefore, the B_{64} bond is thermodynamically favorable site for the adsorption of the FA because of more strain in the 4-MR compared to that in the 6-MR. In other words, the 4-MR has more tendency to react with *trans*-FA molecule, thereby releasing its strain energy through weakening the B_{64} bonds. Based on the NBO analysis, in S case, the B_{64} bond is broken after the adsorption process and increased from 1.98 to 2.45 Å. This adsorption undergoes a hydroxyl-like structural distortion and the FA molecule undergoes structural distortion. The FA-adsorbed atoms are deformed so significantly that an O–H bond in the cluster surface was formed in both of R and S configurations. The O–H bond is twice as long as that in the gas phase. The CO distance on the right side of HCOO becomes 1.30 Å, which is close to the single-bond length of C–O. The distance between H atom and O atom of surface is 1.03 Å, which is close to the standard O–H bond length. This result indicates that the O–H bond of FA should dissociate spontaneously with the formation of a surface OH species, while the adsorbed FO species continues to interact with the surface OH species, as seen from Fig. 5.

To gain a thorough understanding of the changes of electronic properties of $Zn_{12}O_{12}$, it is essential to calculate the density of states (DOS) plots of the tube before and after FA molecule adsorption. From the DOS plot of the bare $Zn_{12}O_{12}$ in Fig. 1, it can be concluded that it is a semiconducting material with a wide E_g of 3.87 eV. Figures 3 and 5 correspond to the DOS of stable configurations of FA-$Zn_{12}O_{12}$. When comparing the DOSs of the free cluster (Fig. 1) system and the adsorbed system, it is found that the presence of FA can slightly decrease the E_g. However, largest change in conduction and valence levels was occurred in configuration R (in which HOMO and LUMO levels move to higher and lower energies, respectively), so E_g of the cluster was decreased from 3.87 to 3.71 eV (4.1 % change).

Adsorption of FO Anion on $Zn_{12}O_{12}$

Next, we examined the stable adsorption geometry and the E_{bin} of the FO on the $Zn_{12}O_{12}$ surface. As candidates for stable geometries, we examined bridging,

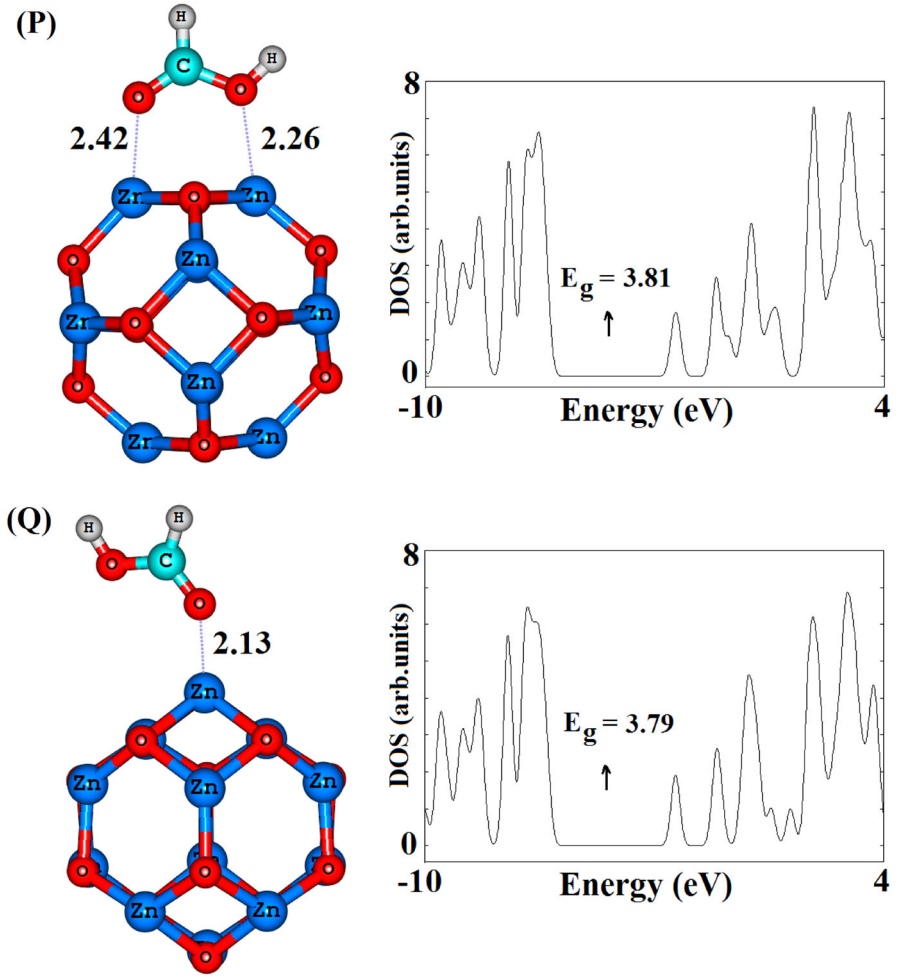

Fig. 3 Optimized geometries of *cis*-FA adsorbed on $Zn_{12}O_{12}$ and their DOS plots. Bond lengths in Å

Table 1 Adsorption energy of FA on cluster (E_{ad} in kcal/mol), HOMO energies (E_{HOMO}), LUMO energies (E_{LUMO}), HOMO–LUMO energy gap (E_g), and Fermi level (E_F) of systems (Figs. 3 and 5) in eV

Configuration	E_{ad}	[a]Q_T (|e|)	E_{HOMO}	E_F	E_{LUMO}	E_g	[b]ΔE_g (%)
$Zn_{12}O_{12}$	–	–	−7.04	−5.10	−3.17	3.87	–
P	−7.37	0.147	−6.51	−4.60	−2.70	3.81	1.5
Q	−11.77	0.311	−6.49	−4.59	−2.70	3.79	2.0
R	−35.81	0.106	−6.98	−5.12	−3.27	3.71	4.1
S	−36.11	0.165	−7.05	−5.14	−3.24	3.81	1.5

[a] Q_T is defined as the average total Mulliken charge on the molecule

[b] Change of E_g of $Zn_{12}O_{12}$ after adsorption

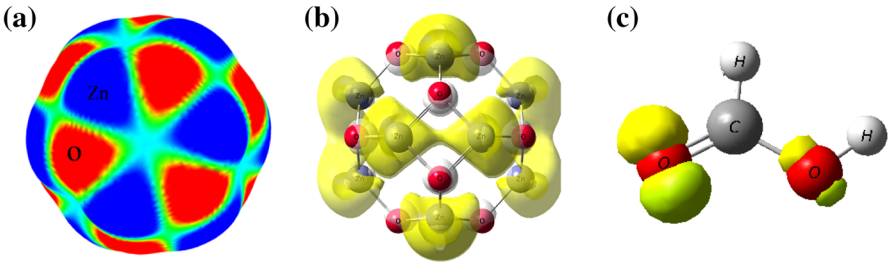

Fig. 4 **a** The calculated molecular electrostatic potential surface **b** the LUMO of $Zn_{12}O_{12}$cluster and **c** the HOMO orbital of FA. The *red color* is referred to the high electron density on oxygen atoms and the *blue one* is referred to the positive sites (Zn atoms) (Color figure online)

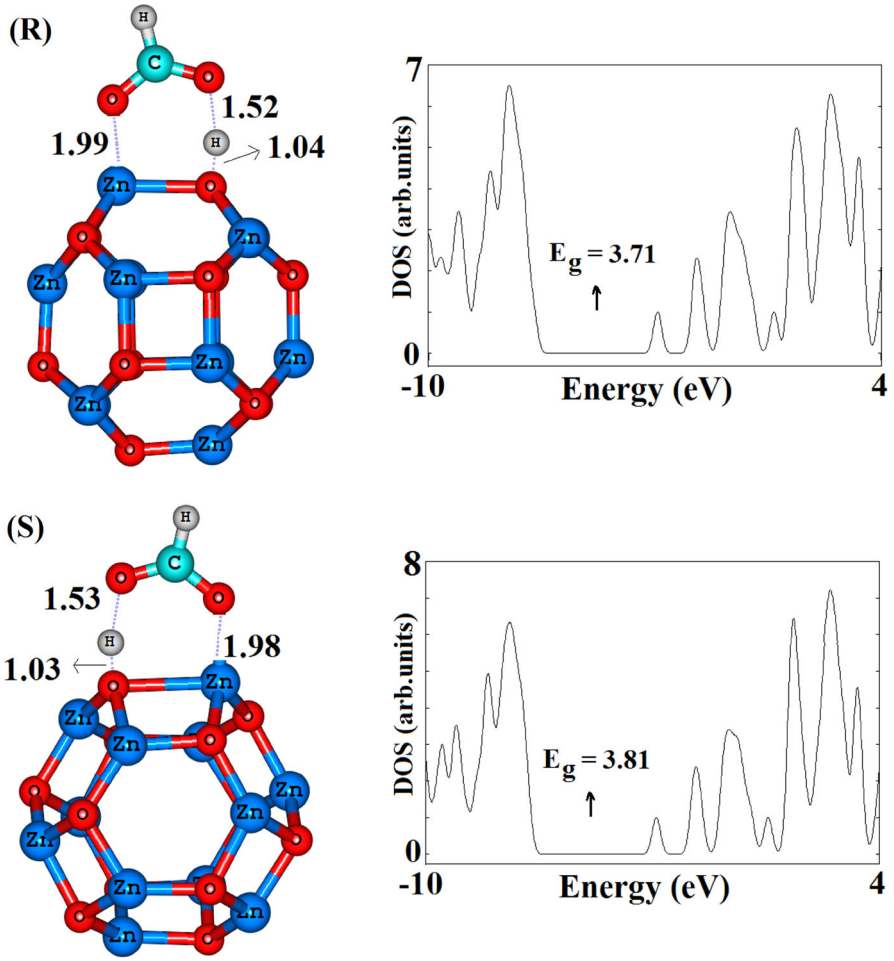

Fig. 5 Optimized geometries of *trans*-FA adsorbed on $Zn_{12}O_{12}$ and their DOS plots. Bond lengths in Å

Table 2 Adsorption energy of FO anion on cluster (E_{ad} in kcal/mol), HOMO energies (E_{HOMO}), LUMO energies (E_{LUMO}), HOMO–LUMO energy gap (E_g), and Fermi level (E_F) of systems (Fig. 6) in eV

Configuration	E_{ad}	Q_T (|e|)[a]	E_{HOMO}	E_F	E_{LUMO}	E_g	ΔE_g (%)[b]
$Zn_{12}O_{12}$	–	–	−7.04	−5.10	−3.17	3.87	–
A	−56.81	−0.490	−3.25	−1.69	−0.14	3.11	19.6
B	−52.58	−0.277	−3.34	−1.71	−0.09	3.25	16.0
C	−50.32	−0.483	−3.58	−2.01	−0.45	3.13	19.1
D	−47.20	−0.424	−3.57	−1.96	−0.36	3.21	17.0

[a] Q_T is defined as the average total Mulliken charge on the molecule

[b] Change of E_g of $Zn_{12}O_{12}$ after adsorption

bidentate, and unidentate structures shown in Fig. 2. In the bridging and bidentate formats, two oxygen atoms interact with Zn atoms, while only one oxygen atom interacts with a Zn atom in the unidentate FO. More detailed information about the simulation of the different FA-$Zn_{12}O_{12}$ systems, including values of E_{ad}, E_g and the charge transfer (Q_T) for these configurations is listed in Table 2. The molecular plane of HCOO is assumed to be perpendicular to the ZnO surface and stands on the Zn atoms.

The optimized geometries for the bridging (configurations **A** and **B**), unidentate (configuration **C**) and bidentate (configuration **D**) are shown in Fig. 6. The configuration A gives rise to an E_{ad} of −56.81 kcal/mol, which is more negative than the E_{ad} values for configurations **B** (−52.58 kcal/mol), **C** (−50.32 kcal/mol) and **D** (−47.20 kcal/mol). The geometries of the bridging structures are almost the same as those of the free FO anion. The OCO angle in the bidentate structure is less than that in bridging and unidentate structures or the free anion. Both bridging and bidentate structures are stabilized by the overlap between the unoccupied s orbital of the Zn atom and the occupied $2p_z$ orbital of the O atom of the FO anion. Each $2p_z$ orbital of the O atom of the FO anion interacts with each s orbital of the Zn atom in the bridging structure, while the one p_z orbital of the O atoms of the FO anion interacts with only one s orbital of the Zn atom in the bidentate structure. The OCO angle in the bidentate structure (**D**) decreases to achieve a greater overlap of these orbitals. This strain in the OCO angle makes the bidentate structure unstable. Note that the HCOO geometry of the unidentate structure (**C**) shown in Fig. 6 is close to that of the free FO anion. The total charges of $HCOO^-$ are −1.000, −0.490, −0.277, −0.483 and −0.424 for the free, bridging **A**, bridging **B**, unidentate **C** and bidentate **D** structures, respectively. Some electron transfer occurs from the FO anion to the surface. Noto et al. suggested that the FO anion assumes a bridging or bidentate structure on the ZnO (1010) surface based on an IR experiment [21]. Our present results suggest that all possible configurations of bridging, unidentate and bidentate structures can exist on the $Zn_{12}O_{12}$ nanocage.

The DOS plots for all adsorption models of FO on $Zn_{12}O_{12}$ have been shown in Fig. 7, indicating that upon the FO chemisorption on the $Zn_{12}O_{12}$, the electronic properties of the cluster have been significantly changed compared to the chemisorption cases. For example, in the most stable configuration (**A**), the DOS

near both of conduction and valence levels have a distinct change compared to that of the pristine cluster, so an impurity electron sate appears at energy level of −3.25 and −0.14 eV after the FO adsorption which would result in the E_g reduction from 3.87 to 3.11 eV. It shows a considerable change of E_g about 0.76 eV (19.6 %), indicating that the electronic properties of the cluster are very sensitive to the adsorption of FO anion.

As shown in Table 2, the E_F is dramatically increased after FO adsorption which indicates that the E_F shifts towards the conduction level. For instance, the E_F is increased from −5.10 to −1.69 eV in most stable FO/$Zn_{12}O_{12}$ complex. However,

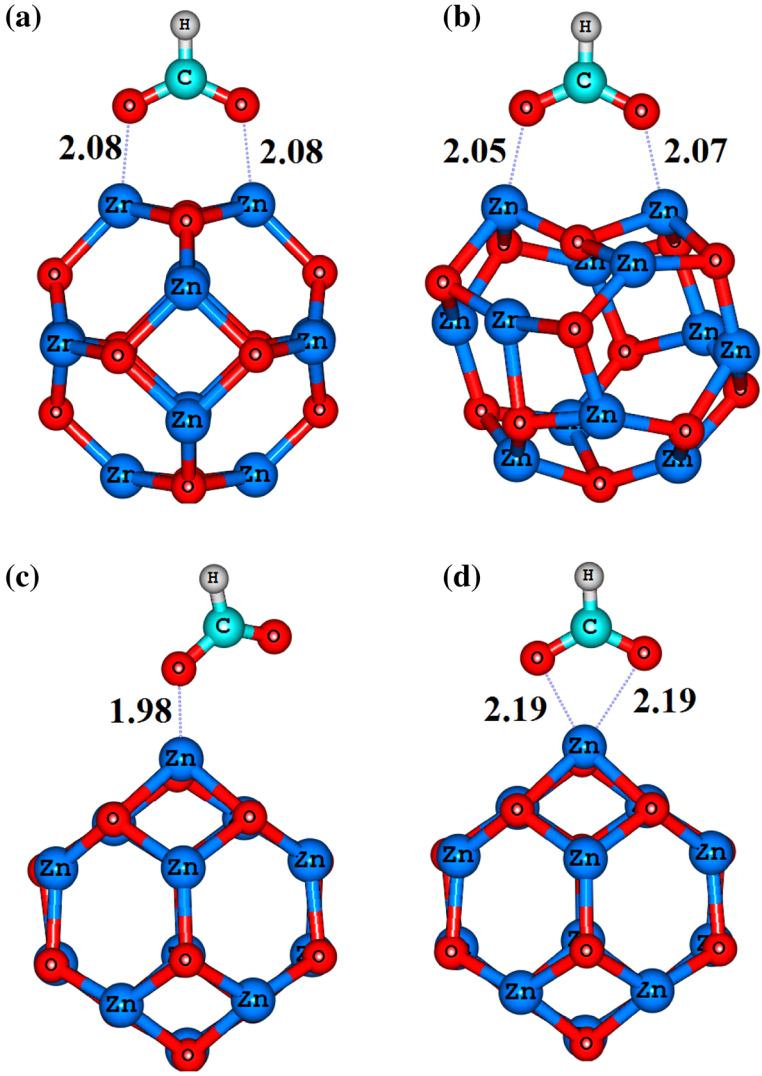

Fig. 6 Optimized geometries of FO anion adsorbed on $Zn_{12}O_{12}$. Bond lengths in Å

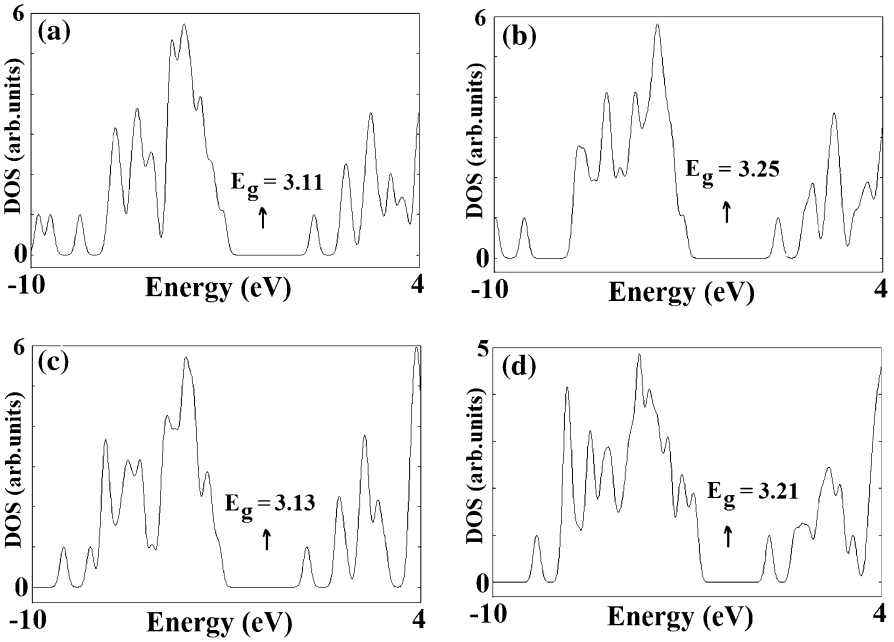

Fig. 7 The DOS plots for different FO -adsorbed $Zn_{12}O_{12}$

Table 3 Dissociation energy of FA on cluster (E_{ad} in kcal/mol), HOMO energies (E_{HOMO}), LUMO energies (E_{LUMO}), HOMO–LUMO energy gap (E_g), and Fermi level (E_F) of systems (Fig. 8) in eV

Configuration	E_{ad}	E_{HOMO}	E_F	E_{LUMO}	E_g	ΔE_g (%)[a]
$Zn_{12}O_{12}$	–	−7.04	−5.10	−3.17	3.87	–
Dis1	−28.08	−6.94	−5.09	−3.24	3.70	4.4
Dis2	−26.76	−6.64	−4.86	−3.09	3.55	8.2

[a] Change of E_g of $Zn_{12}O_{12}$ after dissociation

these phenomena lead to a decrement in the work function that is important in field emission applications. The work function can be computed using the standard procedure by calculating the potential energy difference between the vacuum level and the Fermi level, which is the minimum energy required for one electron to be removed from the Fermi level to the vacuum. The decrement in the work function indicates that the field emission properties of the cluster are facilitated upon the FO adsorption.

Dissociation of FA to FO on $Zn_{12}O_{12}$

Finally, we examined possible routes and mechanisms for the conversion of the FA structure to FO structure on $Zn_{12}O_{12}$. We have probed a number of different adsorption sites on the cluster. However, only two local minima structures were

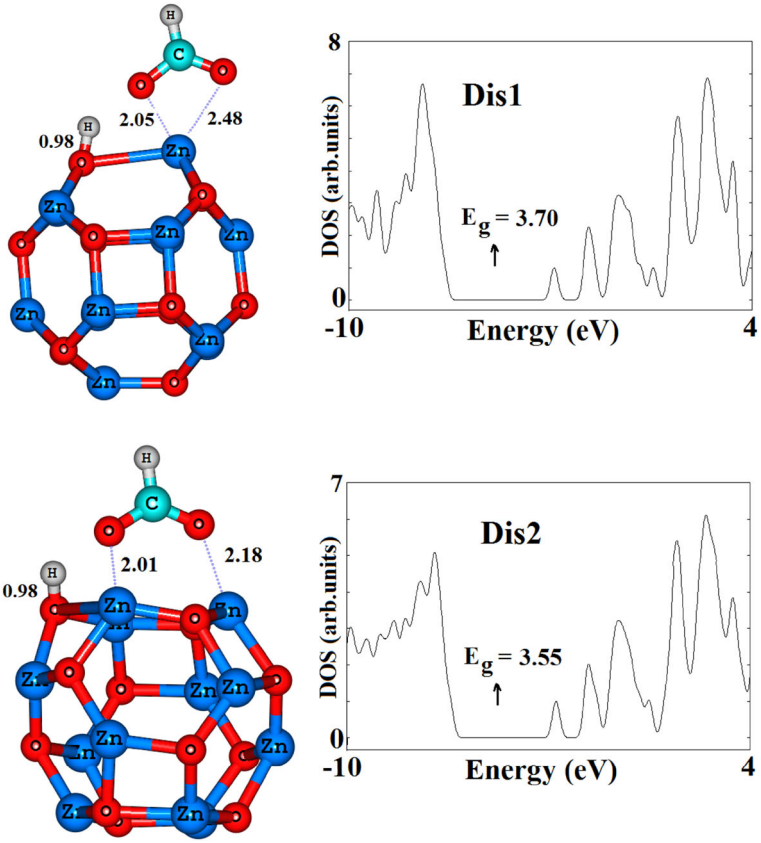

Fig. 8 Optimized geometries of *cis*-FA dissociated on $Zn_{12}O_{12}$ and their DOS plots. Bond lengths in Å

obtained upon the relaxation process (Table 3). In the most stable configuration (**Dis1**, Fig. 8), molecular *cis*-FA from two H atoms is close to O sites of the $Zn_{12}O_{12}$. After relax optimization, the FO anion moves toward the neighboring Zn atom to form a unidentate structure, which is eventually transformed into the bidentate structure. Also, an O–H bond in FA was cleaved and a new O–H bond in $Zn_{12}O_{12}$ surface was formed spontaneously with the distance of 0.98 Å. The OCO angle in **Dis1** configuration is 120° which is slightly lower than bidentate configuration of FO in the cluster (122°). Our transition sate calculations (Fig. 9, **TS1**) show that FA has to overcome an energy barrier about 13.41 kcal/mol to be dissociated within this mechanism.

In the second most stable configuration (**Dis2**, Fig. 8), *trans*-FA was located on the top of 6-MR and after relax optimization FA dissociation was occurred. Unlike former case (**Dis1**), after full optimization, FO anion adsorbed on the cluster as bridging type interaction with two O atoms of cluster and also one O–H bond with the length of 0.98 Å was formed. In the dissociation process of the proton, the $2p_z$ orbital of the surface oxygen donates an electron to the next LUMO of FA, which

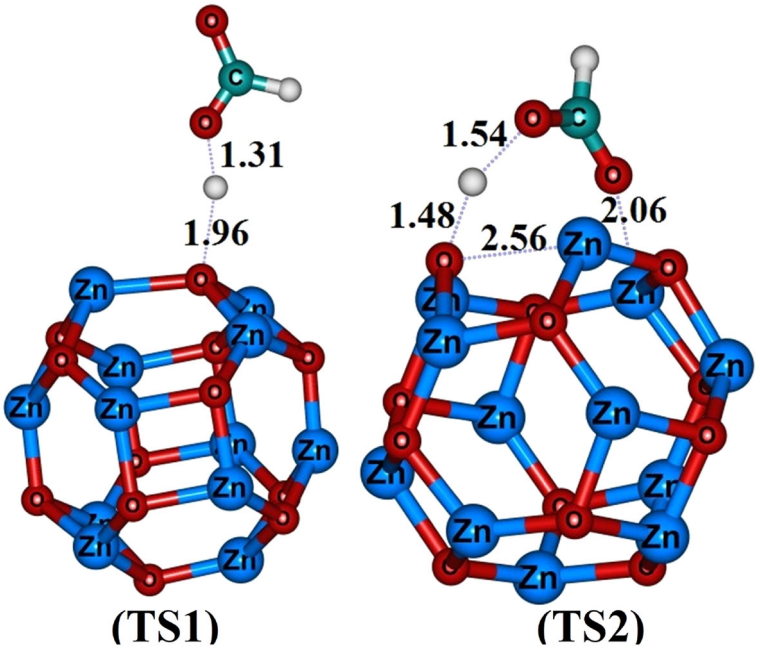

Fig. 9 Transition structures for dissociation of FA to FO anion and H^+ cation. Bond lengths in Å

has an O–H antibonding character. Therefore, the O–H bond of FA is weakened and the surface OH species is formed. Adsorption process in configuration Dis1 ($E_{ad} = -28.08$ kcal/mol) is slightly more favorable than configuration **Dis2** (−26.76 kcal/mol). The favorability of this configuration has been related to the stability of free FA in *cis* and *trans* configurations. Calculated transition state for **Dis2** process (Fig. 9, **TS2**) show that barrier energy is about 17.42 kcal/mol which is somewhat higher than that of **Dis1**.

In the gas phase, *trans*-FA is calculated to be more stable than *cis*-FA by 4.35 kcal/mol. Therefore, dissociation of *cis*-FA on $Zn_{12}O_{12}$ (**Dis1**) is more favorable than *trans*-FA (**Dis2**). From inspection of the DOS plot (Fig. 8), it is revealed that conduction and valence levels of cluster after dissociation of FA is similar to that of the pristine one, and E_g of the cluster slightly reduced to 3.70 and 3.55 eV for **Dis1** and **Dis2** configurations, respectively. The contribution of FA is largely away from the Fermi level. It can be found that $Zn_{12}O_{12}$, after dissociation of FA, are still semiconductors with a wide E_g close to that of the pristine one. In short, chemical dissociation of FA upon $Zn_{12}O_{12}$ can be supposed as a kind of "*harmless modification*".

Conclusion

Adsorption of FA and FO on a $Zn_{12}O_{12}$ nanocage was investigated by means of DFT calculations. The adsorption of *cis*- and *trans*-FAs on the cluster releases

energies in the range of 7.36 to 36.11 kcal/mol with no sensible effect on the electronic properties of the cluster. The adsorption of *trans*-FA was much more favorable than the *cis*-acid and also the *trans*-FA can be dissociated to –H and FO on the cluster surface, releasing energy of 28.08 kcal/mol. Adsorption of FO was much more favorable than FAs. In contrast to FA adsorptions, the FO adsorption significantly influences the electronic properties of the cluster by decreasing the E_g and work function. The decrement in the work function will increase the field electron emission from the cluster surface.

References

1. B. Liu and H. C. Zeng (2003). *J. Am. Chem. Soc.* **125**, 4430.
2. J. Beheshtian, A. A. Peyghan, and Z. Bagheri (2012). *Appl. Surf. Sci.* **258**, 8171.
3. Y. B. Li, Y. Bando, T. Sato, and K. Kurashima (2002). *Appl. Phys. Lett.* **81**, 144.
4. Y. F. Chen, Q. G. Song, and H. Y. Yan (2012). *Comp. Theor. Chem.* **983**, 65.
5. H. Yumoto, T. Inoue, S. J. Li, T. Sako, and K. Nishiyama (1999). *Thin Solid Films* **345**, 38.
6. T. J. Hsueh, C. L. Hsu, S. J. Chang, and I. C. Chen (2007). *Sens. Actuators B Chem.* **126**, 473.
7. D. M. Song, T. H. Wang, and J. C. Li (2012). *J. Mol. Model.* **18**, 5035.
8. C. Wang, S. Xu, L. Ye, W. Lei, and Y. Cui (2011). *J. Mol. Model.* **17**, 1075.
9. A. Peyghan, M. Baei, S. Hashemian, and P. Torabi (2013). *J. Clust. Sci.* **24**, 591.
10. V. Nirmala and P. Kolandaviel (2006). *J. Mol. Struct. THEOCHEM.* **758**, 9.
11. A. Jain, V. Kumar, and Y. Kawazoe (2006). *Comp. Mater. Sci.* **36**, 258.
12. A. Peyghan, M. Baei, M. Moghimi, and S. Hashemian (2013). *J. Clust. Sci.* **24**, 31.
13. S. Xu, M. Zhang, Y. Zhao, B. Chen, J. Zhang, and C. C. Sun (2006). *Chem. Phys. Lett.* **423**, 212.
14. X. D. Gao, X. M. Li, and W. D. Yu (2004). *Appl. Surf. Sci.* **229**, 275.
15. A. Al-Sunaidi and S. Goumri-Said (2011). *Chem. Phys. Lett.* **507**, 111.
16. F. Meshkini, M. Taghizadeh, and M. Bahmani (2010). *Fuel* **89**, 170.
17. H. Onishi, C. Egawa, T. Aruga, and Y. Iwasawa (1987). *Surf. Sci.* **191**, 479.
18. H. Lüth, G. W. Rubloff, and W. D. Grobman (1976). *Solid State Commun.* **18**, 1427.
19. G. C. Cabilla, A. L. Bonivardi, and M. A. Baltanás (2003). *Appl. Catal. A* **255**, 181.
20. L. Kieu, P. Boyd, and H. Idriss (2001). *J. Mol. Catal. A Chem.* **176**, 117.
21. Y. Noto, K. Fukuda, T. Onish, and K. Tamaru (1967). *Trans. Faraday Soc.* **63**, 3081.
22. C. T. Au, W. Hirsch, and W. Hirschwald (1988). *Surf. Sci.* **199**, 507.
23. W. T. Petrie and J. M. Vohs (1991). *Surf. Sci.* **245**, 315.
24. D. B. Lawson and A. Walker (2012). *Comput. Theor. Chem.* **981**, 31–37.
25. V. Bertin, E. Agacino, R. López-Rendon, and E. Poulain (2006). *J. Mol. Struct. THEOCHEM* **769**, 243.
26. A. A. Peyghan, N. Hadipour, and Z. Bagheri (2013). *J. Phys. Chem. C* **117**, 2427.
27. J. Beheshtian, A. A. Peyghan, and Z. Bagheri (2012). *Comput. Mater. Sci.* **62**, 71.
28. M. Moradi, A. A. Peyghan, Z. Bagheri, and M. Kamfiroozi (2012). *J. mol. model.* **18**, 3535.
29. J. Beheshtian, M. T. Baei, A. A. Peyghan, and Z. Bagheri (2012). *J. Mol. Model.* **18**, 4745.
30. M. W. Schmidt, K. K. Baldridge, J. A. Boatz, S. T. Elbert, M. S. Gordon, J. H. Jensen, S. Koseki, N. Matsunaga, K. A. Nguyen, S. Su, T. L. Windus, M. Dupuis, and J. A. Montgomery (1993). *J. Comp. Chem.* **14**, 1347.